Nonlinear Optics, Quantum Optics, Vol. 59, pp. 209–226
Reprints available directly from the publisher
Photocopying permitted by license only

Many-body Reduced Vector Solution and Water Vibrations

A.S. ABDEL-RAHMAN*

Physics Department, Faculty of Science, Cairo University, Egypt

Received: July 30, 2022. Accepted: October 12, 2022.

Reduced mass value and vector are well known for the two-body problem, but the many-body reduced vector problem is not solved yet. The study of many-body problems and their applications (such as vibrational spectroscopy) is one of the more important physical problems. Vibrational spectroscopy provides a powerful tool to perceive the molecular structures and atom motions of molecules. The water molecule is a three-body system stretching vibration that has been previously quantized; their frequencies were defined and showed the infrared (IR) absorption spectrum based on Morse potential. In this work, the reduced mass of the many-body problem is being solved and then used to study the intensity of the stretching vibration modes and show the ratio is in agreement with experiments. The molecule was studied in classical and quantum mechanics to determine its absorption intensity as an example of a reduced mass problem. The results show molecular atomic motions and changes in dipole and reduced mass vector. A Morse-like model for bending was predicted based on the spectroscopic vibration frequency and intensity, defining the bending potential depth of 93.5 kJ/mol.

Keywords: Many-body problem, reduced mass, morse potential, vibration, bending model, water

1 INTRODUCTION

1.1 Two-body system

In classical mechanics, the two-body problem is to predict the motion of two massive objects that are abstractly viewed as point particles. The problem assumes that the two objects interact only with one another; the only force

Corresponding author's e-mail: asabry@sci.cu,edu.eg

affecting each object arises from the other one, and all other objects are ignored.

Let r_1 and r_2 be the vector positions of the two bodies, and m_1 and m_2 be their masses. The goal is to determine the trajectories $r_1(t)$ and $r_2(t)$ for all time t, given the initial positions $r_1(t = 0)$ and $r_2(t = 0)$ and the initial velocities $v_1(t = 0)$ and $v_2(t = 0)$.

When applied to the two masses, Newton's Second Law states that

$$F_{12}\left(r_1, r_2\right) = m_1 \ddot{r}_1 \tag{1}$$

$$F_{21}\left(r_1, r_2\right) = m_2 \ddot{r}_2 \tag{2}$$

where F_{12} is the force on mass 1 due to its interactions with mass 2, and F_{21} is the force on mass 2 due to its interactions with mass 1. The two dots on top of the r position vectors denote their second derivative with respect to time, or their acceleration vectors.

The vector r_{12} (the vector between the two bodies) may be used to rewrite Equations 1 and 2 together as:

$$\ddot{r}_{12} = \ddot{r}_2 - \ddot{r}_1 = \frac{F_{21}}{m_2} - \frac{F_{12}}{m_1} \tag{3}$$

The centre of mass, which is affected by all body masses, is written globally as:

$$\sum_{i=1}^{n} m_i \left(r_i - r_{cm}\right) = 0 \tag{4}$$

and is equal to:

$$r_{cm} = \frac{\sum_{i=1}^{n} m_i r_i}{\sum_{i=1}^{n} m_i} \tag{5}$$

According to Newton's first law, the forces F_{12} and F_{21} are equal in magnitude and opposite in directions, so Equ. 3 may be written:

$$\ddot{r}_{12} = F_{21}\left(\frac{1}{m_2} + \frac{1}{m_1}\right) = \frac{F_{21}}{\mu} \tag{6}$$

where μ is the reduced mass and can be written as follows for n-bodies globally:

$$\frac{1}{\mu} = \sum_{i=1}^{n} \frac{1}{m_i} \tag{7}$$

The problem is that for an n-body system, the division of total forces in the system by the system's reduced mass equals the second derivative of the reduced mass vector with respect to time. In a two-body system, the reduced mass vector is that between these bodies, but in a higher-body system, this vector is not defined.

1.2 Molecular vibrations of water

Water molecule structure and vibration modes are discussed in many works. According to the group theory character table, the structure of the water molecule is a C_{2v} molecule (Table 1) with three vibration modes in the liquid case: (a) A_1 symmetric stretching mode at 3656.65cm^{-1} with 0.07 relative intensity, (b) B_1 asymmetric stretching mode at 3755.79cm^{-1} with 1.00 relative intensity, and (c) A_1 symmetric bending mode at 1594.59cm^{-1} with 1.47 relative intensity [1-7].

The infrared transmittance spectroscopy for vapour [10-15], liquid water [10, 16, 17] and ice [18-21] are reported and show the dependence of absorption lines on the temperature.

The rest structure of the water molecule according to ref [1-3], origin set at centre of mass (cm) below the oxygen atom at 0.065Å and above the hydrogen atoms at 0.521Å on the z-axiz. Both hydrogen atoms are located 0.757Å to the right and left of the z-axis. From here on out, the hydrogen atom located on the negative side of the x-axis will be denoted by H_1 and the atom on the positive side will be denoted by H_2.

1.3 Morse potential

The separation between the hydrogen and oxygen atoms (r_e) is 0.957Å, with a Morse potential [22-27] (Equ. 8) of dissociation energy (D_d) and an O-H bond of 424.67kJ/mol [28, 29] is controlled by two coefficients; barrier depth

TABLE 1
C_{2v} character table [8, 9].

C_{2v}	E	C_2 (z)	σ_v(xz)	σ_v(yz)	linear functions and rotations	Quadratic functions
A_1	+1	+1	+1	+1	z	x^2, y^2, z^2
A_2	+1	+1	-1	-1	R_z	xy
B_1	+1	-1	+1	-1	x, R_y	xz
B_2	+1	-1	-1	+1	y, R_x	yz

(D) and potential width (a), which are related to the force constant ($k = \mu\omega^2$: ω the angular frequency and equal to $2\pi\nu_0$) as written in Equ. 9.

$$V = D\left(e^{-2a(r-r_e)} - 2e^{-a(r-r_e)}\right) \tag{8}$$

$$a = \sqrt{\frac{k}{2D}} \tag{9}$$

The quantum solution of Morse potential eigenvalues (E_n) is discovered as described in Equ. 10, while $n = 0,1,2,\ldots$, which determines the eigenstates, begins with the ground state $n = 0$ and proceeds to successive states $n > 0$ [30-32]. The quantum ground state (E_0) is slightly larger than the classical ground state (D).

$$E_n = h\nu_0\left(n+\frac{1}{2}\right) - \frac{1}{4D}\left(h\nu_0\left(n+\frac{1}{2}\right)\right)^2 - D \tag{10}$$

$$\nu_0 = \frac{a}{2\pi}\sqrt{\frac{2D}{\mu}} \tag{11}$$

$$\Delta E_n = E_{n+1} - E_n = h\nu_0 - (n+1)\frac{(h\nu_0)^2}{2D} \tag{12}$$

1.4 Quantum harmonic oscillator

Although the simple harmonic oscillator is not applicable to spectroscopic potentials due to the anharmonicity found in real molecules, this potential was studied as an approximation in this work.

Equation 13 can be used to express the potential of a quantum harmonic oscillator. The solution of these potential eigenvalues (E_n) is found as described in Equation 14, as that of Morse One, but the harmonicity appears clearly where the difference between any two successive eigenstates is constant. The quantum ground state (E_0) is also larger than the classical ground state (D).

$$V = \left(\frac{1}{2}k\left(r-r_e\right)^2\right) - D = \left(2\pi^2\mu\nu_0^2\left(r-r_e\right)^2\right) - D \tag{13}$$

$$E_n = h\nu_0\left(n+\frac{1}{2}\right) - D \tag{14}$$

The barrier depth of the harmonic oscillator is deeper than dissociation energy by ($\frac{1}{2}h\nu_0$) and the intercept of classical and quantum potentials is located at r_n; and can be written as:

$$\delta_n = r_n - r_e = \pm\sqrt{\frac{2h\nu_0}{k}\left(n+\frac{1}{2}\right)} = \pm\sqrt{\frac{h}{2\pi^2\mu\nu_0}\left(n+\frac{1}{2}\right)} \tag{15}$$

where δ_n is the change in the O-H bond length.

1.5 Classical and quantum mechanics

The forces between macroscopic systems are restricted by the classical equations of motion. This application is ideal because quantum mechanics equations, as well as the application of this mechanics to this range, are extremely difficult to solve. Going from the microscopic to the atomic level, the motion of electrons around the nucleus cannot be explained by classical mechanics, while quantum mechanics and its main point of quantized energy levels are the appropriate consideration for this level.

Many scientists believe that these two mechanics systems are actually the same, but this system is closer to the classical one for macroscopic ranges and the quantum one for microscopic ranges. One can imagine combining these two mechanics systems between these scales, such as the interatomic scale.

Harmonic oscillators are one of the important problems in mechanics. These oscillators can be found at the molecular level as vibrational interatomic atoms. The interpretation of these oscillator energies can be considered from either a classical or quantum perspective. In contrast to classical mechanics, which describes continuous energies, quantum mechanics depicts discrete energy levels. The disparity between these solutions to the same problem can be interpreted as a measurement agreement.

The quantum mechanics solution illustrates an energy level starting with ground level E_0 and rising to successive higher levels. The transitions between these levels are governed by selection rules. According to classical fact, all atoms vibrate (at the ground energy level) continuously until they reach absolute zero temperature. At this temperature, one cannot expect the stopping of the motion of electrons around the nucleus where they obey quantum mechanics, but the stopping of vibrations is possible where it is classically interpretative.

From the quantum solution, the ground's vibrational energy level is located over the barrier potential. This difference can be linked to classical thermal energy as follows:

$$\left(E_0 - D\right) = \left(D_d - D\right) \propto k_B T \tag{16}$$

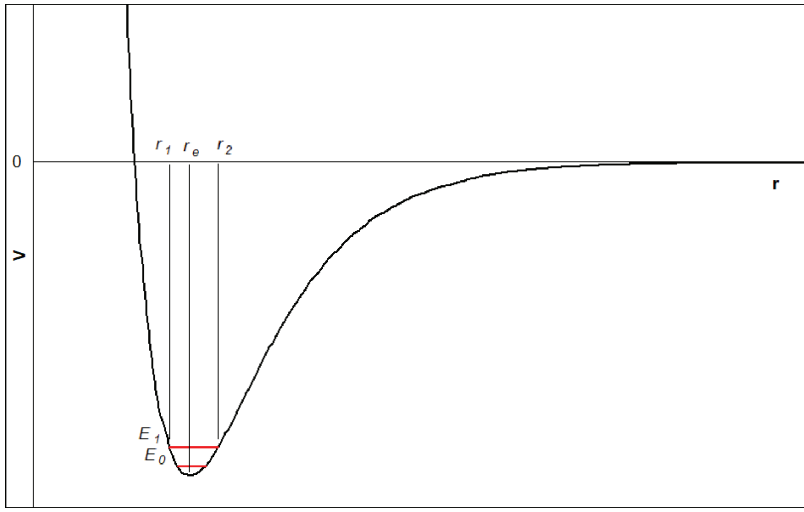

FIGURE 1
Morse potential and amplitudes r_1 and r_2.

where k_B is the Boltzmann constant, where the amplitude of oscillation is a classical view, and the total energy of the oscillator system E_t (the sum of potential and kinetic energies) should meet the potential at the amplitude of oscillation (typically r_1 and r_2 in Fig. 1). From the point of view of quantum mechanics, there is no definite oscillation amplitude, but there is a probability of finding the particle of a certain length, Δr equal to the square of the eigenfunction.

The convergence between classical and quantum mechanics in the interatomic vibrations is to consider the oscillator total energy E_t equal to the quantized energy level E_1 and hence intercepting at the oscillation amplitudes r_1 and r_2 in Fig. 1. So, the vibration oscillator energy will be treated as a quantum problem, while the vibration amplitude will be solved classically.

The zero temperature case makes the barrier depth equal to the ground energy level with zero vibrational amplitude ($r_1 = r_2 = r_e$). This scenario is acceptable to discuss the vibrational modes of molecules.

Upon this assumption, the barrier width a and transition energy (and thus frequency ν_0) should be temperature-dependant. This also agrees with the experimental measurements of the IR transmittance spectra of water.

The IR vibration is caused by a change in the separation of the negative charge (the oxygen ion) from the net positive charge (midway between the two hydrogen ions) in the molecule. From this point, the importance of discussing the atomic locations through vibration is clear.

In this work, the n-body system's reduced mass vector is discussed, and the three vibration modes of water (as an example of a three-body prob-

lem) are also discussed by classical and quantum solutions, their intensities, and atom motion vectors. The total potential of the water molecule in this work is taken as the summation of the Morse potentials between H_1-O and H_2-O, while the weak Van der Waals potential between hydrogen atoms will be neglected (its values are very small compared to the Morse potential).

2 METHODOLOGY

2.1 Many-body system

To expand the two-body system to many body system, first of all, the force F_{21} in Equ. 6 will be replaced by the sum of all forces between each pair of bodies. After that, how to define the reduced mass vector?

To solve this question, the two-body unequally reduced mass vector can be written as:

$$r_{12} = r_2 - r_1 = \left(r_2 - r_{cm}\right) - \left(r_1 - r_{cm}\right) \tag{17}$$

The reduced mass vector direction always takes one of the r_1 and r_2 directions (may be the larger one). According to this point, the unit vector of the reduced mass vector $\hat{r}_{12}$ can be written as:

$$\hat{r}_{12} = \frac{\left(r_2 - r_{cm}\right) + \left(r_1 - r_{cm}\right)}{\left|\left(r_2 - r_{cm}\right) + \left(r_1 - r_{cm}\right)\right|} \tag{18}$$

and can be written globally as:

$$\hat{r} = \frac{\sum_{i=1}^{n}\left(r_i - r_{cm}\right)}{\left|\sum_{i=1}^{n}\left(r_i - r_{cm}\right)\right|} \tag{19}$$

Now, one should differentiate between the reduced mass vector's magnitude and direction $\hat{r}_{12}$. Its magnitude is the summation of the magnitudes of the vectors from the two bodies to the centre of mass. Then Equ. 17 can be written in terms of $\hat{r}_{12}$ as:

$$r_{12} = \left(r_2 - r_{cm}\right) - \left(r_1 - r_{cm}\right) = \left(\left|r_2 - r_{cm}\right| + \left|r_1 - r_{cm}\right|\right)\hat{r}_{12} \tag{20}$$

and can be written globally as:

$$r = \left(\sum_{i=1}^{n} \left| r_i - r_{cm} \right| \right) \hat{r} = \frac{\sum_{i=1}^{n} \left| r_i - r_{cm} \right|}{\left| \sum_{i=1}^{n} \left(r_i - r_{cm} \right) \right|} \sum_{i=1}^{n} \left(r_i - r_{cm} \right) \tag{21}$$

This is the n-body system's reduced mass vector; its second time derivative equals the summation of all forces in the system divided by the system's reduced mass.

3 RESULTS AND DISCUSSION

3.1 Vibration and center of mass

According to the definition of vibration in molecules, the centre of mass is reserved. Where the movement of the centre of mass is achieved through vibration and rotation operations, this is solved by introducing the translation of molecules alongside the operations.

Herein, the centre of mass conservation sets two main equations for all vibration modes:

$$m_O Z'_O + m_H \left(-Z'_{H1} - Z'_{H2} \right) = 0 \tag{22}$$

$$m_O X'_O + m_H \left(-X'_{H1} + X'_{H2} \right) = 0 \tag{23}$$

The Z and X are the subscripted atoms' locations, the prime over the location parameters refer to the location via vibration, and the unprimed parameters refer to the rest of the molecule, and they are written in the introduction section.

The vibration operation is divided into some modes: stretching, bending (in-plane and out of plane), twisting, scissoring, and rocking. The fact that each of these modes is active alone means that the stretching vibration requires the changing of bond lengths without changing the bond angles [9, 33-35], and so on.

3.2 Symmetric stretching vibration of water

According to the C_{2v} character table, the A_1 symmetric stretching vibration of water can be characterized. This vibration mode conserves all symmetry elements. This mode of vibration allows both hydrogen atoms to go away from

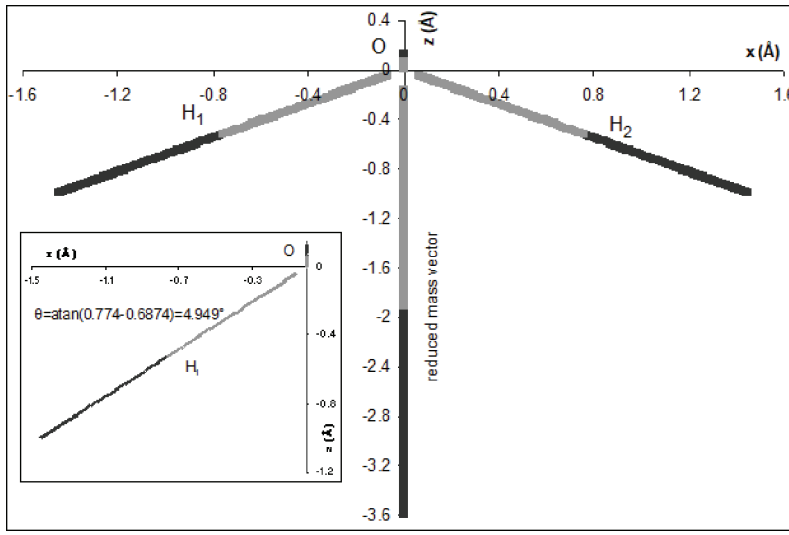

FIGURE 2
The water A_1 symmetric stretching vibration.

the oxygen atom by the same displacement (δ) ($Z'_{H1} = Z'_{H2}$ and $X'_{H2} = -X'_{H1}$) and, of course, the oxygen atom goes up on the z-axis to conserve the centre of mass ($X'_O = 0$). Also, the angle between O-H_1 and O-H_2 vectors is conserved, so the atomic motions of hydrogen atoms incline by about 5° (as shown in Figure 2, inset figure, where this motion path passes the origin or centre of mass) on the vector between oxygen and hydrogen atoms.

Figure 2 illustrates the water molecule's symmetric stretching vibration A_1 along with the atomic motions and reduced mass vector. The darker points represent the stretching, while the lighter points represent the compression motion. If the H_1 and H_2 atoms move away from the oxygen atom in the mentioned direction by displacement (δ), all the atoms' equations of motion in terms of δ are listed in Table 2 beside the reduced mass vector *r* and the dipole length *d*.

While both O-H bonds have synchronised motions, the total system potential has double the O-H dissociation energy as the ground state of the Morse potential, so:

$$\mu\ddot{r} = F = -\frac{\partial V}{\partial r}\hat{r} \tag{24}$$

or in scalar form

$$\ddot{\delta} = \frac{4aD}{1.9877\mu}\left[e^{-2a\delta} - e^{-a\delta}\right] \tag{25}$$

TABLE 2
A_1 symmetric stretching vibration atomic motions.

Atom	Description
H_1	$(-0.7569 - 0.7908\delta)x + (-0.5203 - 0.5436\delta)z$
H_2	$(0.7569 + 0.7908\delta)x + (-0.5203 - 0.5436\delta)z$
O	$(0.065554 + 0.068486\delta)z$
$\|r\|$	$(-1.9026 - 1.9877\delta)$
$\|d\|$	$(0.58587 + 0.6121\delta)$

This deferential equation may be solved numerically to get the function $\delta(t)$. But the importance of this problem is to get the values of D and a of the total system potential, which can be calculated by means of the eigenstates of the potential as follows:

$$-2D_d = E_0 = \frac{1}{2}h\nu_0 - \frac{1}{16D}\left(h\nu_0\right)^2 - D \tag{26}$$

$$h\nu_{sy.str.} = \Delta E_0 = h\nu_0 - \frac{\left(h\nu_0\right)^2}{2D} \tag{27}$$

$$\nu_0 = \frac{a}{2\pi}\sqrt{\frac{2D}{\mu}} \tag{28}$$

where $\nu_{sy.str.}$ the frequency of the symmetric stretching vibration of water molecules ($=1.096 \times 10^{14}$Hz). The solution of the Morse potential parameters (Figure 3) was achieved numerically and is listed in Table 3.

The IR vibration active mode is a result of the change of molecule dipole moment (or dipole length) through the vibration process.

As shown in Table III, the atomic vibration frequency and barrier potential are slightly larger than the symmetric stretching vibration frequency and double the dissociation energy, respectively. The reduced mass vector vibration amplitude has anharmonicity due to the oscillation's unequal displacements.

3.3 Asymmetric stretching vibration of water

The B_1 asymmetric stretching vibration of water conserves the xz mirror and totally loses the C_2 fold axis and xy mirror plane. This mode of vibration allows one hydrogen atom to go away from the oxygen atom while the other one moves towards the oxygen atom by the same displacement (δ) and, of course, the oxygen atom moves parallel to the x-axis to conserve the centre of

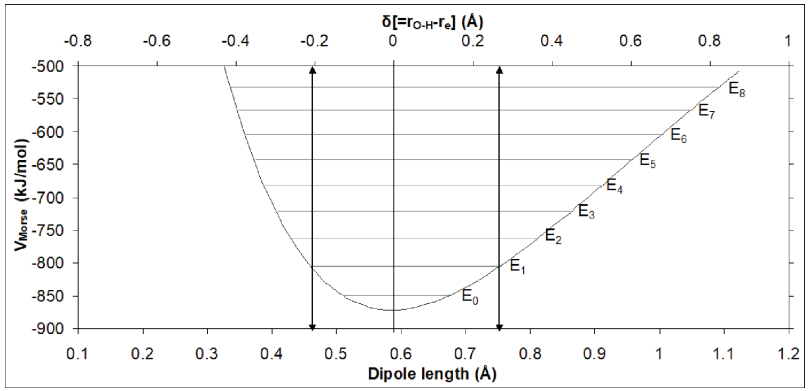

FIGURE 3
The water A_1 symmetric stretching vibration potential.

TABLE 3
A_1 symmetric stretching vibration parameters of water.

Parameter	Description	Value	Unit
ν_0	Atomic vibration frequency	1.1252×10^{14}	Hz
D	Barrier potential	871.66	kJ/mol
k	Vibration force constant	4.055×10^{2}	N/m
a	Barrier width	1.1835×10^{10}	m^{-1}
h_{min}	O-H minimum vibration bond length	0.75	Å
h_{max}	O-H maximum vibration bond length	1.228	Å
Δr	Reduced mass vector vibration amplitude	0.5387 – 0.4115	Å
Δd	Dipole length vibration amplitude	0.1659 – 0.1267	Å

mass ($Z'_O = 0$). The angle between O-H_1 and O-H_2 vectors is conserved in any stretching vibration.

Figure 4 illustrates the water molecule's asymmetric stretching vibration B_1 along with the atomic motions and reduced mass vector. The hydrogen atom moves in a straight line at an angle of nearly 5.57° (as shown in the inset figure of Figure 8), on the vector between oxygen and hydrogen atoms.

Table 4 shows the equation of motion of each atom beside the reduced mass vector under the influence of the hydrogen atom vibration amplitude (δ). One can notice that both the reduced mass vector and the dipole length are directly proportional to the square of the hydrogen vibration amplitude.

Since the motion of hydrogen atoms is out of phase (one atom moves towards the oxygen atom while the second one moves away), the sum of their O-H Morse potentials is close to the harmonic oscillator. This harmonic oscil-

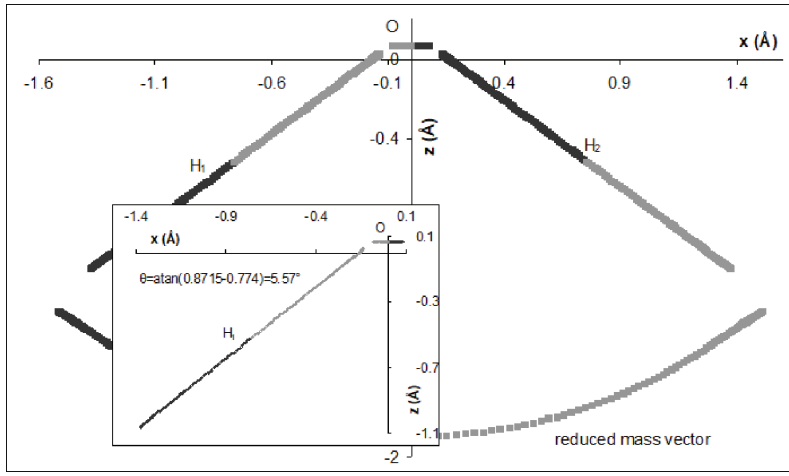

FIGURE 4
The water B_1 asymmetric stretching vibration.

TABLE 4
B_1 asymmetric stretching vibration atomic motion.

Atom	Description
H_1	$(-0.7569 + 0.7023\delta)x + (-0.5203 + 0.6121\delta)z$
H_2	$(0.7569 + 0.7023\delta)x + (-0.5203 - 0.6121\delta)z$
O	$(-0.08848\delta)x + (0.065554)z$
$\|r\|$	$(1.90259 + 0.08623\delta^2)$
$\|d\|$	$(0.58587 + 0.04734\delta^2)$

lator depth should be double the O-H depth. The ground state energy (which equals the double of dissociation energy) should be larger than this depth by ($\frac{1}{2}h\nu_0$) and the separation between two successive energy states is quantized ($h\nu_0$). The total potential of this system should be written as:

$$V_{tot} = D\left(e^{-2a\delta} + e^{2a\delta} - 2e^{-a\delta} - 2e^{a\delta}\right) \approx \frac{k'}{2}\delta^2 - 2D \tag{29}$$

where k' denotes the system's vibration force constant, which differs from the Morse potential force constant (mentioned in Equ. 9). After applying the spectroscopic coefficient ($\nu_0 = 1.126 \times 10^{14}$ Hz), the potential depth D and the force constant k' are calculated to be 871.816 kJ/mol and 4.06×10^2 N/m, respectively.

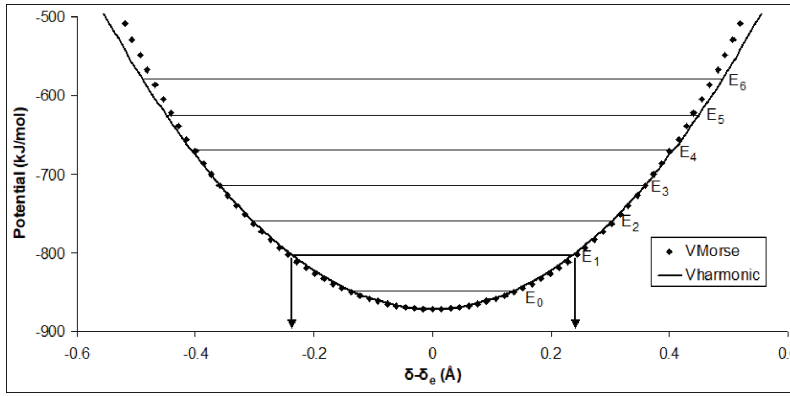

FIGURE 5
The water B_1 asymmetric stretching potential.

The harmonic potential of this vibration (continuous curve in Figure 5) can be fitted to subtract two identical Morse potentials (dots curve in Figure 5), and then the Morse potential width a fitted to be 1.13×10^{10} m^{-1}. The first six energy levels are set on the same figure, and E_1 intercepts the potential at ±0.2348Å. Thus, the changes in reduced mass vector and dipole length are 0.00475Å and 0.0238Å, respectively.

The ratio of the dipole length change to the change in the reduced mass vector between symmetric and asymmetric vibrations is 0.0615:1. This ratio should represent the intensity of the experimental IR absorption lines and is found in good agreement with them [3, 36].

3.4 Symmetric bending vibration of water

The A_1 symmetric bending vibration of water conserves all symmetry elements by synchronising the scissor motion of the hydrogen atoms while the oxygen atom moves on the z-axis to keep the centre of mass at the origin. Let's define θ_e as the equilibrium bond angle; the vibration is mainly associated with the difference between the bond angle and its equilibrium value while the bond length is constant. Figure 6 illustrates the water molecule's symmetric bending vibration A_1 along with the atomic motions and reduced mass vector. Table 5 shows these motions with respect to $\varphi = (\theta - \theta_e)$.

There is a definite potential model for bending [37-40], In this work; a simple model for bending is presented that resembles Morse potential in its shape. In bending vibration, while the bond lengths being constant, the effective term in the potential is directly proportional to φ (instead of δ in stretching modes). The potential is really affected by the arc length in front of the bond angle, so the term should be written as $r_e\varphi$, and then the potential equation may be written as:

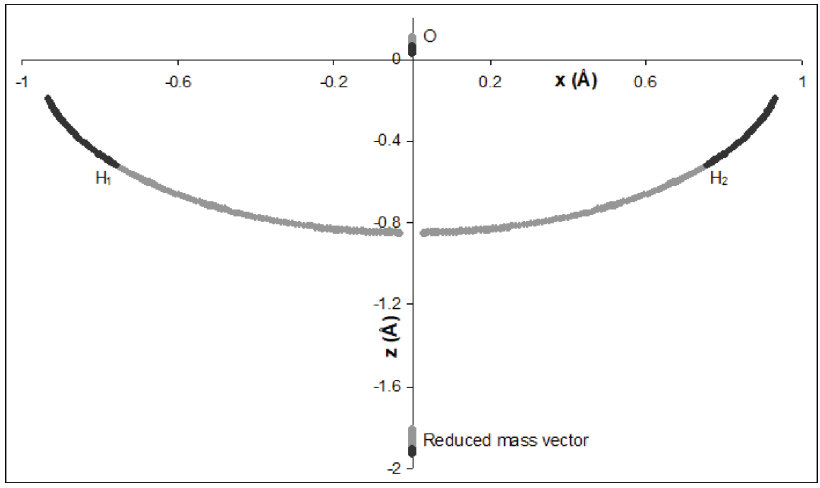

FIGURE 6
The water A_1 symmetric bending vibration.

TABLE 5
A_1 symmetric bending vibration atomic motions.

Atom	Description
H_1	$(-0.75693-0.2808\varphi+0.0814\varphi^2)x-(-0.5203-0.324\varphi-0.0735\varphi^2)z$
H_2	$(0.75693-0.2808\varphi-0.0814\varphi^2)x-(-0.5203-0.324\varphi-0.0735\varphi^2)z$
O	$(0.065553-0.0408\varphi-0.0093\varphi^2)z$
$\|r\|$	$(1.902594-0.0462\varphi-0.0107\varphi^2)$
$\|d\|$	$(0.58587-0.3648\varphi-0.0827\varphi^2)$

$$V = D\left(e^{-2ar_e\varphi} - 2e^{-ar_e\varphi}\right) \tag{30}$$

where both coefficients a and D still have their earlier definitions. Once applying the spectroscopic vibration frequency (4.78×10^{13} Hz) and taking into account that the IR absorption line intensity should be 1.47 times the B_1 stretching line, the dipole change to reduced mass vector change should be 7.365, and then the angle difference should be 0.2276 rad. This value is the intercept of the potential equation with the E_1 energy state. Hence, one can estimate the potential barrier width and depth as shown in Table 6.

The water-bending potential model is being predicted and shown in Figure 7. The reason why the difference between ground state energy (29 kJ/mol) and potential depth is larger than that between ground and first energy states is the nearness between the vibrating energy (165.5 kJ/mol) and the barrier depth.

TABLE 6
A_1 symmetric bending vibration parameters of water.

Parameter	Description	Value	Unit
ν_0	Atomic vibration frequency	4.147×10^{14}	Hz
D	Barrier potential	93.51	kJ/mol
k	Vibration force constant	5.507×10^{3}	N/m
a	Barrier width	1.332×10^{11}	m^{-1}
θ_{min}	H-O-H minimum vibration bond angle	101.55	°
θ_{max}	O-H maximum vibration bond angle	117.56	°
Δr	Reduced mass vector vibration amplitude	1.8994 – 1.9147	Å
Δd	Dipole length vibration amplitude	0.6053 – 0.4961	Å

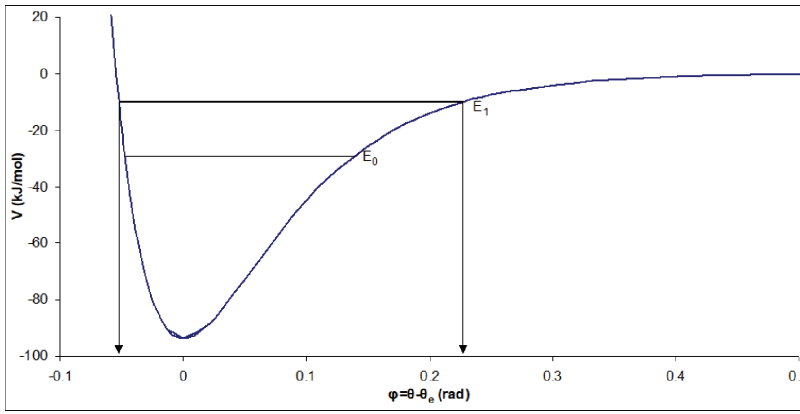

FIGURE 7
The water bending potential model.

CONCLUSIONS

Calculating the reduced mass vector is essential for describing the atomic motions of molecules and estimating the dipole moment, which describes the IR absorption of the molecule through vibration modes. The work shows the reduced mass vector of the many-body problem. Quantum and classical mechanics are used side by side to describe the vibration mechanisms in water molecules, which show the relative intensity of the IR absorption lines of water too close to the measured lines. The reason for the very high absorption of the B_1 asymmetric stretching of water was clear, due to its higher stretching hormoticity than others. A novel prediction of the bending potential was presented and illustrates that the bending potential depth of water is 93.5 kJ/mol.

Conflict of Interest
The authors declare no conflict of interest.

Data Availability Statement
The datasets generated during and/or analyzed during the current study are available from the corresponding author on reasonable request.

REFERENCES

[1] Eisenberg D., and Kauzmann W. (1969), *The Structure and Properties of Water*, London, Oxford University Press.
[2] Headrick J.M., Diken E.G., Walters R.S., Hammer N.I., Christie R.A., Cui J., Myshakin E.M., Duncan M.A., Johnson M.A., and Jordan K.D. (2005), Spectral signatures of hydrated proton vibrations in water clusters, *Science*, 308, 1765-1769, DOI: 10.1126/science.1113094.
[3] Cui H., Zhang X.B., Su J.F., Yang Y.X., Fang Q., and Wei X.Y. (2015), Vibration–rotation absorption spectrum of water vapor molecular in frequency selector at 0.5–2.5 THz range, *Optik*, 126, 3533-3537, DOI: 10.1016/j.ijleo.2015.08.066.
[4] Abdel-Aal S.K., and Abdel-Rahman A.S. (2017), Synthesis, structure, lattice energy and enthalpy of 2D hybrid perovskite [NH3(CH2)4NH3]CoCl4, compared to [NH3(CH2)nNH3]CoCl4, n=3–9, *J. Cryst. Grow*., 457, 282-288, DOI: 10.1016/j.jcrysgro.2016.08.006.
[5] Abdel-Aal S.K., Abdel-Rahman A.S., Kocher-Oberlehner G.G., Ionov A., and Mozhchil R. (2017), Structure, optical studies of two-dimensional hybrid perovskite for photovoltaic applications, *Acta Cryst*., A73, C1116, DOI: 10.1107/S2053273317084583.
[6] Moubarak D.I., Hassan H.H., El-Rasasi T.Y., Ayoub H.S., Abdel-Rahaman A.S., Khairy S.A., and Elbashar Y. (2018), Measuring the Internal Friction for Some Rubbers Doped Nano Carbon by Laser Shadowgraphic Technique, *Nonlinear Optics and Quantum Optics*, 49(3-4), 295-310.
[7] Elbashar Y.H., Omran A.E., Khaliel J.A., Abdel-Rahaman A.S., and Hassan H.H. (2018), Ultraviolet Transmitting Glass Matrix for Low Power Laser Lens, *Nonlinear Optics and Quantum Optics*, 49(3-4), 247-265.
[8] Elbashar Y.H., Hussien S.M., Khaliel J.A., Moubarak D.I., Abdel-Rahaman A.S., and Hassan H.H. (2018), Optical spectroscopic analysis of sodium zinc phosphate glass doped Ccadmium oxide used for laser window protection, *Annals of the University of Craiova, Physics*, 28, 57-72.
[9] Abdel-Rahman A.S. (2020), Group theory character table enhancement by introducing the partial molecular symmetry principle in the molecular spectroscopy, *Egy. J. Sol*., 42, 35-48, DOI: 10.21608/EJS.2020.148110.
[10] https://webbook.nist.gov/chemistry, NIST: National Institute of Standards and Technology.
[11] Hassan H., Moubarak D., Khaliel J., Ayoub H., Abdel-Rahaman A., Khairy S., El-Rasasi T., and Elbashar Y. (2018), Design and Construction of Optical Laser Shadowgraphy System for Measuring the Internal Friction of High Elasticity Solids, *Nonlinear Optics and Quantum Optics*, 48(4), 313-320.
[12] Abdel-Aal S.K., and Abdel-Rahman A.S. (2019), Fascinating Physical Properties of 2D hybrid perovskite [(NH3)(CH2)7(NH3)]CuClxBr4-x, x = 0, 2 and 4, *J. Elect. Mat*., 48(3), 1686-1693, DOI: 10.1007/s11664-018-06916-7.
[13] Abdel-Aal S.K., Abdel-Rahman A.S., Gamal W.M., Abdel-Kader M., Ayoub H.S., El-Sherif A.F., Fawzy M., Bozhko S., Yakimov E.E., and Yakimov E.B. (2019), Crystal Structure, Vibrational Spectroscopy, and Optical Properties of 1D - Organic-Inorganic Hybrid Perovskite of [NH3CH2CH(NH3)CH2]BiCl5, *Acta Cryst*., B75(5) 880-886, DOI: 10.1107/S2052520619011314.

[14] Dalby F.W., and Nielsen H.H. (1956), Infrared Spectrum of Water Vapor. Part I—The 6.26μ Region, *J. Chem. Phys*., 25, 934, DOI: 10.1063/1.1743146.

[15] Kandeel M.F., Abdel-Aal S.K., El-Sherif A.F., Ayoub H.S., and Abdel-Rahman A.S. (2019), Crystal Structure and Optical Properties of 1D-Bi based Organic-Inorganic Hybrid Perovskite, *IOP Conf. Ser*., 610, 012063, DOI: 10.1088/1757-899X/610/1/012063.

[16] Elbashar Y.H., Rashidy W.A., Khaliel J.A., Moubarak D.I., Abdel-Rahaman A.S., and Hassan H.H. (2020), Optical Spectroscopic Study of Hard Ultraviolet Protection Sunglasses, *Nonlinear Optics and Quantum Optics*, 51(3-4), 171-193.

[17] Elbashar Y.H., Ibrahem R.A., Khaliel J.A., Moubarak D.I., Abdel-Rahaman A.S., and Hassan H.H. (2020), Optical Spectroscopic Analysis of Bandpass Absorption Glass Filter Based on Vanadium Copper Oxide for Laser Safety Applications, *Nonlinear Optics and Quantum Optics*, 51(3-4), 195-212.

[18] Zelent B., and Vanderkooi J.M. (2009), Infrared spectroscopy used to study ice formation: The effect of trehalose, maltose, and glucose on melting, *Analy. Biochem*., 390(2) , 215-217, DOI: 10.1016/j.ab.2009.04.019.

[19] Moubarak D.I., Hassan H.H., Ayoub H.S., El-Rasasi T.Y., Khairy S.A., Elbashar Y.H., and Abdel-Rahaman A.S. (2019), Measuring the Internal Friction of Butadiene Acrylonitrile Rubber (NBR) Doped Nanocarbon Using the Laser Shadowgraphy Pulse Excitation Technique, *Lasers in Engineering*, 43(4-6), 319-328.

[20] Moubarak D.I., Khaliel J.A., El-Rasasi T.Y., Ayoub H.S., Abdel-Rahaman A.S., Khairy S.A., Hassan H.H., and Elbashar Y.H. (2019), Mechanical and laser shadowgraphy studies of nanosized carbon black loaded natural rubber, *Lasers in Engineering*, 43(4-6), 201-212.

[21] Abdel-Aal S.K., and Abdel-Rahman A.S. (2020), Graphene influence on the structure, magnetic and optical properties of rare-earth perovskite, *J. Nanopart. Res*., 22(9), 267, DOI: 10.1007/s11051-020-05001-7.

[22] Morse P.M. (1929), Diatomic Molecules According to the Wave Mechanics. II. Vibrational Levels, *Phys. Rev*., 34(1), 57, DOI: 10.1103/PhysRev.34.57.

[23] D. Shi-Hai, Lemus R., and Frank A. (2001), Ladder operators for the Morse potential, *Int. J. Quant. Chem*., 86(5), 433-439, DOI: 10.1002/qua.10038.

[24] Matej P., Dušanka J., and Janez M. (2004), Temperature Dependence of Water Vibrational Spectrum: A Molecular Dynamics Simulation Study, *J. Phys. Chem.*, A108(50), 11056-11062, DOI: 10.1021/jp046158d.

[25] Moubarak D.I., Hassan H.H., El-Rasasi T.Y., Ayoub H.S., Abdel-Rahaman A.S., Khairy S.A., and Elbashar Y.H. (2021), Internal Friction of Nano-Sized Carbon Black-Loaded Polymeric Composites Using Laser Shadowgraphic Technique: A Review, *Nonlinear Optics and Quantum Optics*, 53(1-2), 31-59.

[26] Elbashar Y.H., Omran A.E., Hussien S.M., Mohamed M.A., Ibrahem R.A., Rashidy W.A., Abdel Rahaman A.S., and Hassan H.H. (2020), Molecular and Spectroscopic Analysis of Zinc Oxide Doped Sodium Phosphate Glass, *Nonlinear Optics and Quantum Optics*, 52(3-4), 337-347.

[27] Abdel-Aal S.K., Ismail S.H., and Abdel-Rahman A.S. (2020), New Synthesis route of lead-free hybrid graphene nanoparticles, *Egy. J. Sol*., 42, 49-59, DOI: 10.21608/EJS.2020.148111.

[28] Abdel-Aal S.K., Kandeel M.F., El-Sherif A.F., and Abdel-Rahman A.S. (2021), Synthesis, Characterization and Optical Properties of New Organic-Inorganic Hybrid Perovskites [(NH3)2(CH2)3]CuCl4 and [(NH3)2(CH2)4]CuCl2Br2, *Phys. Stat. Sol*., A218(12), 2100036, DOI: 10.1002/pssa.202100036.

[29] Elbashar Y.H., Rashidy W.A., Khaliel J., Hussien S.M., Omran A.E., Ibrahem R.A., Mohamed M.A., Abdel Rahaman A.S., and Hassan H.H. (2021), Molecular Spectroscopic Analysis of Sodium Phosphate Zinc Copper Glass Matrix Doped Magnesium, *Nonlinear Optics and Quantum Optics*, 54(3-4), 205-215.

[30] Elbashar Y.H., Ibrahem R.A., Khaliel J., Hussien S.M., Omran A.E., Rashidy W.A., Mohamed M.A., Abdel-Rahaman A.S., and Hassan H.H. (2021), Infrared Spectroscopy Analysis of Vanadium Oxide Doped Sodium Zinc Phosphate Glass Matrix, *Nonlinear Optics and Quantum Optics*, 54(3-4), 231-239.

[31] Abdel-Aal S.K., Beskrovnyi A.I., Ionov A., Mozhchil R.N., and Abdel-Rahman A.S. (2021), Structure investigation by Neutron Diffraction and X-ray diffraction of Graphene Nanocomposite CuO-rGO prepared by low cost method, *Phys. Stat. Sol*., A218(12), 2100138, DOI: 10.1002/pssa.202100138.

[32] Elbashar Y.H., Hussien S.M., Khaliel J., Mohamed M.A., Omran A.E., Ibrahem R.A., Rashidy W.A., Abdel Rahaman A.S., and Hassan H.H. (2021), Infrared Spectroscopic Analysis of Cadmium Doped Sodium Zinc Phosphate Glass Matrix, *Nonlinear Optics and Quantum Optics*, 54(1-2), 105-114.

[33] Abdel-Aal S.K., Abdel-Rahman A.S., Bortel G., Pekker Á., Kamaras K., and Faigel G. (2021), Fascinating structure and physical properties of lead-free hybrid perovskites for multifunctional applications, *Acta Cryst*., A77, C754, DOI: 10.1107/S0108767321089431.

[34] Abdel-Rahman A.S. (2022), Fascinating Physical Properties of Multi-functional Materials: A Review, *Nonlinear Optics Quantum Optics*, in press.

[35] Abdel-Rahman A.S. (2022), A semi-empirical approach model for neo-Hookean solids, *Inter. J. Comp. Meth. Eng. Sci. Mech*., in press, DOI: 10.1080/15502287.2022.2113184.

[36] Abdel-Rahman A.S., Abdel-Aal S.K., Faigel G., Kamaras K., Gábor B., and Pekker A. (2021), Vibrational spectroscopy as a confirmation method for structural analysis, *Acta Cryst*., A77, C956, DOI: 10.1107/S0108767321087432.

[37] Abdel-Aal S.K., Bortel G., Pekker Á., Kamarás K., Faigel G., and Abdel-Rahman A.S. (2022), Structure investigation and vibrational spectroscopy of two prospective hybrid perovskites based on Mn and Co, *J. Phys. Chem. Sol*., 161, 110400, DOI: 10.1016/j.jpcs.2021.110400.

[38] Ronald P.B. (1933), The application of quantum mechanics to chemical kinetics, *Proceedings of the Royal Society,* A139(838) 466-474, DOI: 10.1098/rspa.1933.0031.

[39] G. Tarczay, and Császár A.G. (1999), The barrier to linearity of water, *J. Chem. Phys*., 110(24), 11971, DOI: 10.1063/1.479135.

[40] Zobov N.F., Shirin S.V., Polyansky O.L., Tennyson J., Coheur P.-F., Bernath P.F., Carleer M., and Colin R. (2005), Monodromy in the water molecule, *Chem. Phys. Lett*., 414(1-3) 193-197, DOI: 10.1016/j.cplett.2005.08.028.